Research on Engineering Structures & Materials
www.jresm.org
Research Group

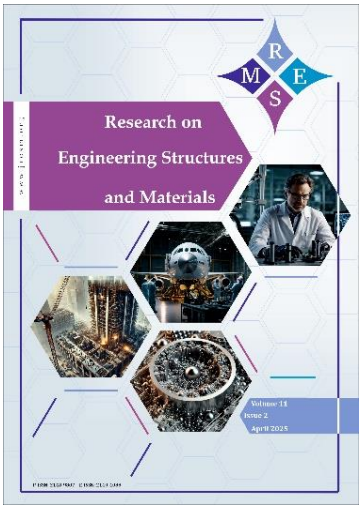

Investigation of electro-mechanical and corrosion behavior of leaded copper

Md Hasan Ruhan Rabbi, Md Abdur Rahaman, Fatema Akter, Md Mezbah Uddin

Online Publication Date: 20 July 2025

URL: http://www.jresm.org/archive/resm2025-767me0318rs.html
DOI: http://dx.doi.org/10.17515/resm2025-767me0318rs

Journal Abbreviation: *Res. Eng. Struct. Mater.*

To cite this article
Rabbi M H R, Rahaman M A, Akter Fatema, Uddin M M. Investigation of electro-mechanical and corrosion behavior of leaded copper. *Res. Eng. Struct. Mater.*, 2025; 11(6): 3245-3260.

Research on Engineering Structures & Materials
www.jresm.org
Research Group

Research Article

Investigation of electro-mechanical and corrosion behavior of leaded copper

Md Hasan Ruhan Rabbi [1,a], Md Abdur Rahaman [2,b], Fatema Akter [1,c], Md Mezbah Uddin [*,1,d]

[1]*Department of Naval Architecture and Marine Engineering, Military Institute of Science and Technology, 1216, Dhaka, Bangladesh*
[2]*Department of Computer Science and Engineering, BRAC University, 1212, Dhaka, Bangladesh*

Article Info

Article History:

Received 18 Mar 2025

Accepted 15 July 2025

Keywords:

Old/waste copper;
Pb inclusion;
Tensile behavior;
Hardness;
Conductivity;
Sea-water corrosion;
Microstructure

Abstract

Copper (Cu) is a well-known high-conductive material with good mechanical strength, machinability, corrosion resistance, and wear resistance. As such, Cu is widely used in industries, automobiles, aircraft, and marine applications as electrical connectors, piping systems, fittings, and heat exchanger tubes, among others. The presence of lead (Pb) in copper, widely known as leaded copper, does not behave exactly in the same manner as pure copper. Unfortunately, Pb inclusion as a trace amount in copper has not been considered by researchers and has remained neglected so far. Therefore, the present paper is an attempt to investigate the electro-mechanical and corrosion behavior of leaded copper. The mechanical properties are significantly affected by the presence of lead content. However, the impact on electrical conductivity is comparatively less pronounced than the changes observed in mechanical properties. Additionally, the microstructure demonstrates a notable geometric effect, varying with the different percentages of lead present. A progressive surge in the corrosion rate as the lead content in copper alloys increases is also found to be significant and can also be found through OEM images.

1. Introduction

Silver, gold, aluminum, and copper are among the most widely recognized materials known for their excellent conductivity. Among these, copper and its alloys stand out as the most commonly used due to their exceptional electrical and thermal conductivity, adequate strength, corrosion resistance, machinability, formability, and wear resistance. These properties make copper highly sought after for use in electrical wires, components, and system parts across commercial, industrial, and marine sectors [1,2]. With rapid advancements in science and technology, alongside economic growth, the global demand for copper continues to rise steadily.

Consequently, there is an increasing focus on recovering copper from old or discarded products due to the dwindling availability of natural copper ores [3]. After extended operational use, waste electrical wires and electronic equipment (WEEE) present two options: recycling copper through intricate and costly extraction processes to restore properties close to the original state or reusing the discarded materials as they are for suitable engineering applications. While recycling ensures properties akin to new copper, it involves significant expense and complexity. Conversely, reusing waste copper is much cheaper, but the associated functional properties need to be thoroughly assessed to identify appropriate engineering applications [4–6]. Therefore, understanding and

*Corresponding author: mezbah@name.mist.ac.bd
[a]orcid.org/0009-0005-0742-8127; [b]orcid.org/0009-0007-4036-3147; [c]orcid.org/0009-0003-2896-8363; [d]orcid.org/0000-0001-7750-7625
DOI: http://dx.doi.org/10.17515/resm2025-767me0318rs

characterizing the functional properties of old copper is of great practical relevance to facilitate its reuse.

Copper wires and machine parts retrieved from various sources, such as buildings, industries, and ship-breaking operations, often contain trace amounts of soldering materials like lead and tin. Over time, copper and its alloys may also absorb lead (Pb) from their operational and environmental conditions [7]. Although the lead content in such cases is usually minimal, its influence on the electro-mechanical properties & corrosive nature of copper cannot be overlooked [8,9]. Numerous research studies have been conducted globally on various seas and gulfs, including the seawater of the Peruvian Port [10], seawater systems on the Norwegian Continental Shelf [11], tropical island seawater [12], and the Gulf of Mexico [13] among others. While each study presents unique findings and observations relevant to their specific regions, the Bay of Bengal has not received sufficient attention for observing the effects trace lead inclusion in copper. Thus, it becomes essential to examine how varying percentages of lead affect copper's behavior.

In this context, the present study aims to investigate such properties of leaded copper. To simulate the impact of lead on waste or old copper sourced from various applications, sample materials will be developed by casting copper with controlled lead content in the range of 1% to 8%.

2. Methods and Material

2.1. Material Preparation

Since lead and tin are the most promising copper-based alloys due to their adsorption tendency over their lifespan [1], to ascertain the influence of lead presence on copper i.e. from 0% to 8% Cu-Pb-based alloys were produced and experimented. In this context, pure lead and copper are collected from the local market by verifying their chemical purity. To facilitate identification, the pure copper sample was designated as Material-I, while the Cu-1%Pb, Cu-2%Pb, Cu-4%Pb, and Cu-8%Pb alloys were labeled as Materials-II, III, IV, and V, respectively. Material-I was procured directly in its as-cast condition from the industry, whereas Materials-II to V were developed through controlled casting where the presence of lead is controlled with the order of 2, i.e., the amount of lead is 2^0, 2^1, 2^2, 2^3 percent against the remaining copper percentage. After developing four materials, their chemical compositions were examined using the X-ray fluorescence (XRF) spectrometer of model Olympus DPO-2000-CC, and the corresponding results found are presented in Table 1.

Table 1. Mass density and chemical composition of the materials under study (mass fraction %)

Elements	Material-I pure Cu	Material-II Cu-1Pb	Material-III Cu-2Pb	Material-IV Cu-4Pb	Material-V Cu-8Pb
Cu	99.65	98.88	97.93	96.03	91.95
Pb	-	1.12	2.07	3.97	8.05
ρ(g/cm^2)	8.94	8.96	8.99	9.04	9.13

After determining the chemical compositions, the materials were shaped into various sizes suitable for experimentation using a Computerized Numerical Control (CNC) milling machine. Meticulous machining was performed to minimize the impact on surface grains. Samples were prepared in dog-bone shapes measuring 92.15 x 6 x 3 mm with a gauge length of 33 mm, adhering to ASTM standards for tensile property testing. Additionally, square samples measuring 15 x 15 x 3 mm were prepared to facilitate the evaluation of micro-hardness, electrical conductivity, and microstructural properties.

2.2. Experimental Details

The research methodology employed in this study is illustrated in Fig. 1, outlining the process from the conceptual phase to the final outcomes.

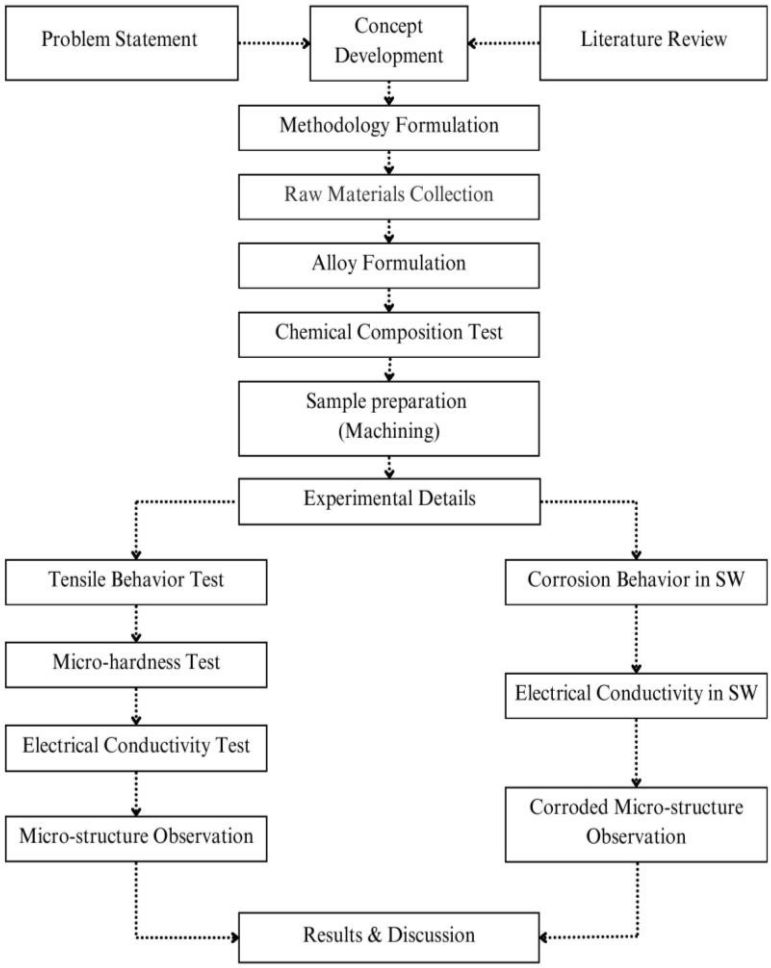

Fig. 1. Workflow diagram of experimental procedure

2.2.1. Tensile Behavior

The reuse of old or recycled copper plays a critical role in technological advancements and economic development. Consequently, characterizing the tensile properties of such materials becomes a priority. The tensile behavior of the samples was assessed using a universal testing machine (Model: Shimadzu UH-F1000 KNX). The presence of lead in recycled copper remains a significant factor of interest during tensile characterization. Although the quantities of soldering materials such as lead and tin in old or scraped copper may be minimal, their influence on tensile properties is considerable.

Copper's cubic crystal structure provides it with exceptional ductility and malleability. However, incorporating lead in varying amounts can disrupt the crystal structure by introducing dislocations, potentially altering the material's mechanical properties [14]. These changes may impact the material's strength and highlight its potential for use in specific applications where lead-contaminated scrap copper could serve as a cost-efficient alternative.

A total of 20 specimens, representing all five material groups, were prepared following the ASTM E8 standard for tensile testing. These samples were systematically categorized for experimental evaluation. Tensile tests were conducted to analyze the influence of lead content on various parameters, including ultimate tensile strength, yield strength, Young's modulus, fracture strength, toughness, and both elastic and plastic strains.

2.2.2. Micro-Hardness

During its operational lifespan, old or scrap copper often absorbs trace amounts of lead from its surrounding environment, which can result in the degradation of key properties, including hardness. Microhardness testing assesses a material's ability to resist deformation on a localized

scale. However, the limited understanding of the hardness characteristics of leaded copper in its residual state restricts its use to ordinary applications rather than more advanced engineering purposes. Therefore, determining the hardness of leaded copper is essential for exploring its potential for higher-value reuse applications. To assess the microhardness of the five study materials, square specimens were mechanically ground in sequential stages using silicon carbide (SiC) emery papers with grits of 160, 300, 600, 900, 1200, 1500, and 1800. After the dry grinding process, the specimens were wet polished with alumina paste and dried using an air blower at room temperature.

Microhardness tests were performed using a computer-interfaced Micro Vickers Hardness Tester (Model: TM HV-1000DTE) in compliance with the ASTM E384-10e2 standard. The test involved pressing a square-based diamond-shaped Vickers pyramid indenter into the specimen's surface. An applied force of 1000 gf was maintained for 10 seconds during each test. The interaction between the indenter and the material resulted in a permanent surface deformation or indentation, the dimensions of which were measured using a microscope. The measured diagonal of the indentation, combined with the applied load, was used to calculate the Vickers hardness value. Fifteen readings were taken at different locations on each of the five samples to ensure data reliability. The Vickers hardness (H_v) was determined using Eq (1):

$$H_v = \frac{1854.4 * \mathrm{P}}{d^2}\ kgf/mm^2 \tag{1}$$

where, H_v: Stress, P: Load applied in gf, d: Mean diagonal length of the indentation in μm [15].

2.2.3. Electrical Conductivity

Copper is widely recognized as one of the most commercially utilized materials due to its excellent electrical and thermal conductivity, making it ideal for various applications involving the transfer of electricity and heat. However, the effect of introducing soldering elements such as lead on copper's conductivity remains largely unexplored. Understanding how lead contamination influences conductivity is essential for identifying potential reuse applications of lead-affected copper. Electrical conductivity measurements were performed using an Electric Conductivity Meter (Model: TMD-101) with a precision of ±0.1% IACS (International Annealed Copper Standard). Initially, the conductivity of the samples was tested to establish baseline values before exposing them to a seawater environment. Subsequently, repeated measurements were taken at specific time intervals over a 36-day period of seawater immersion to observe any variations caused by corrosion. To ensure accuracy and reliability, each sample was tested at least ten times.

2.2.4. Micro-Structure

The microstructural analysis was conducted using an optical-electronic microscope (OEM), model BW-S500. Sample surfaces were first polished with silicon carbide (SiC) abrasive paper of progressively finer grit sizes: 180, 300, 600, 900, 1200, 1500, and 1800. Following the dry polishing process, the samples underwent wet polishing using alumina paste in conjunction with a water flow, and they were subsequently rinsed with acetone. After completing surface preparation, the samples were etched with a hydrogen peroxide (H_2O_2) solution. OEM micrographs were captured for all five materials, both before and after etching, to analyze their microstructures. Additionally, after a 36-day immersion in seawater, the microstructures of corroded samples were re-examined without etching to pinpoint the areas most affected by corrosion, as presented in Fig. 7.

2.2.5. Corrosion Effect in Seawater Environment

Seawater is widely recognized as a potent corrosive medium due to its composition, which includes a complex electrolyte mixture of highly concentrated salts, organic matter, suspended particles, and dissolved gases [16]. The seawater in the Bay of Bengal, as outlined in Table 2, reflects similar characteristics [17,18]. Despite being a member of the noble metal family, copper materials are not entirely resistant to corrosion in such an aggressive environment, resulting in weight loss per unit of exposed surface area over the immersion period [1,19–21].

Table 2. Contents and properties of sea water used for investigation

Parameter	Unit	Concentration Present	Analysis Method
pH	-	7.14	pH meter
Total dissolved solids (TDS)	mg/L	28000	Conductivity meter
Total suspended solids (TSS)	mg/L	48	UVS
Turbidity	mg/L	21000	Titrimetric
Sulfate (SO_4^{2-})	mg/L	1320	UVS
Dissolved oxygen	mg/L	7.29	DO meter
Electric conductivity	µS/cm	48000	Conductivity meter

To evaluate the corrosion behavior of scrap copper in a seawater environment, 50 liters of seawater were collected from Off Moheskhali Fairway Buoy (coordinates: Latitude 21°25.45' N, Longitude 20°37.82' E) in Bangladesh. This study examined the corrosion characteristics of scrap copper using the gravimetric method, which involves monitoring changes in the mass of test coupons over time while submerged in the collected seawater under static conditions. For the experimental setup, a Sartorius Entris 224-1S weighing machine (featuring a 90 mm pan diameter and a maximum weighing capacity of 220 g, with a precision of 0.1 mg) and a CG100 ABDL ultrasonic thickness gauge (measurement resolution: 0.01 mm) were employed. Measurements were recorded at specific time intervals after 1, 3, 6, 12, 18, 24, and 36 days of immersion. The degradation of mass per unit exposed surface area and the corresponding corrosion rates for each testing phase were computed using Eq (2) and Eq (3) respectively. Mass degradation of sample coupon:

$$\Delta W = \frac{W_o - W_f}{A}\ mg/cm^2 \tag{2}$$

The rate of corrosion:

$$R_{corr} = \frac{k * \Delta W}{\rho * T}\ mm/yr \tag{3}$$

where, ΔW: Mass degradation against exposed surface area in mm/cm^2, W_o: Initial mass in g, W_f: Mass measured during the investigation phase after a specific duration of submersion in g, A: Surface area of the exposed sample in the medium in cm^2, R: Corrosion rate in mm/yr, K: Unit conversion factor, ρ: Coupon material density in g/cm^3, T: Submerged phase duration in hour [22].

3. Measured Results and Discussions

3.1. Leading Effect on Tensile Behavior

The load-deflection characteristics are investigated through the standard tensile test of the copper and its leaded alloy samples, and results have been presented in Fig. 2. Here, the UTS values of pure copper in cast condition are found to be 279 MPa. The inclusion of only 1% lead in pure Cu reduces the UTS by 34.46%. Similarly, with the inclusion of 2%, 4%, and 8% lead, the UTS reduces by 41.6%, 52.19%, and 60.62%, respectively.

For pure Cu, the Young's Modulus is found to be 830.90 MPa, which reduces by 25.84%, 31.44%, 33.75%, and 32.38% with the presence of lead at 1%, 2%, 3%, and 4%, respectively. The yield strength of pure copper is found to be 271 MPa, showing a significant drop of 69.99%, 69.60%, 73.81%, and 73.88% due to the similar inclusion. Similar behavior is also found in fracture strength, which is measured to be 93.48 MPa for pure Cu and reduces by 49.39%, 47.75%, 53.17%, and 49.61% due to the corresponding percentages of lead present as shown in Fig. 2. The reduction in Tensile strength and Young's modulus with increasing Pb content in Cu–Pb alloys is primarily due to the metallurgical incompatibility between copper and lead. Owing to its extremely low solubility in the Cu matrix, lead forms soft, non-load-bearing inclusions that act as stress concentrators, reducing the alloy's mechanical performance [23]. These lead particles often localize at grain boundaries, disrupting microstructural integrity and encouraging early plastic

deformation and failure [24]. Furthermore, the weak interfacial adhesion between Pb and Cu facilitates debonding under mechanical stress, which further contributes to the reduction in both stiffness and strength [25]. The substantial difference in elastic moduli—Pb versus Cu, also leads to a pronounced decrease in overall stiffness as Pb content increases [26].

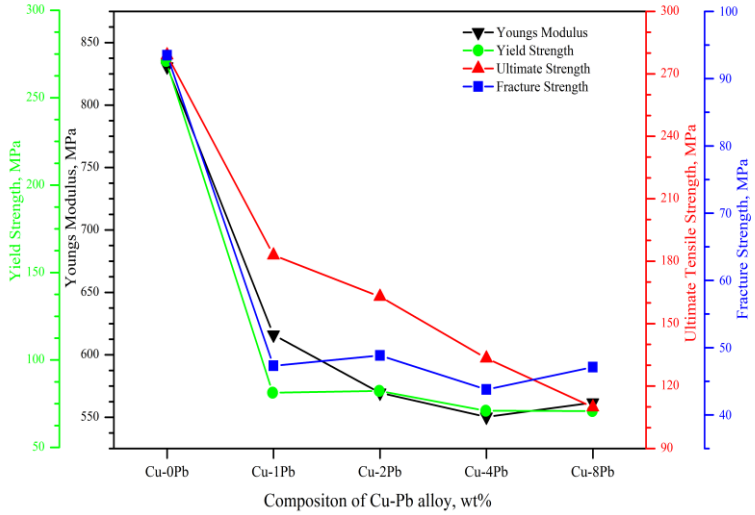

Fig. 2. Young Modulus & Tensile Strength Curves for Different Compositions of Cu-Pb Alloy

Different strain values have been illustrated in Fig. 3. In pure Cu, the elastic strain is found to be 0.324%, which reduces significantly in the presence of only 1% Pb. As the lead presence increases to 2%, 4%, and 8%, the elastic strain fluctuates by a negligible amount. On the contrary, the plastic strain of pure Cu was 9.80%, which increased to 10.78% and 9.98% with 1% and 2% Pb presence, respectively. However, it decreased to 7.23% and 4.50% with the addition of 4% and 8% Pb, respectively. The total strain level of the materials shows a similar behavior as the plastic strain.

The strain behavior of Cu–Pb alloys is influenced by the immiscibility of lead in the copper matrix. At low Pb contents, the introduction of soft Pb particles reduces elastic strain due to the disruption of the continuous Cu lattice. These inclusions create weak interfaces that impair elastic deformation capacity [1,27]. Plastic strain initially increases due to the lubricating effect of finely dispersed Pb, which facilitates dislocation motion. However, with higher Pb content, the formation of course Pb agglomerates promotes stress concentration and crack initiation, leading to a reduction in plastic and total strain [28,29].

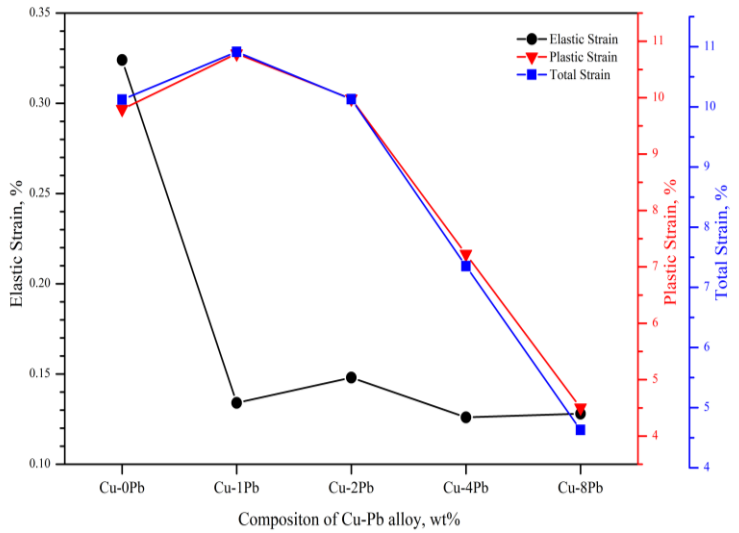

Fig. 3. Strain rate curves for different compositions of Cu-Pb alloy

The material toughness variation due to the variable composition of lead has been analyzed and is presented in Fig. 4. For pure Cu, it is found to be 24.76x10^6 J/m^3 which shows a significant reduction of 38.29%, 46.53%5, 68.94%, and 85.10% due to the presence of 1%, 2%, 4%, and 8% Pb respectively.

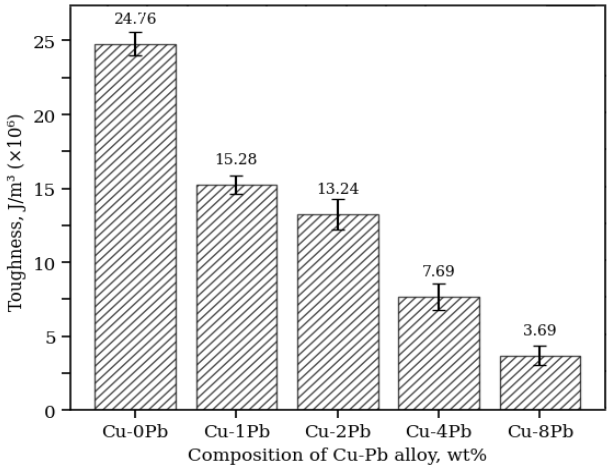

Fig. 4. Toughness variation for different compositions of Cu-Pb alloy

3.2. Leading Effect on Micro-Hardness

Measured micro-hardness values of all five samples were taken 15 times in different locations for greater reliability and standard deviation (SD) was calculated and illustrated in Fig. 5. For pure Cu, the micro-hardness value is found to be 75.65 gf/mm^2 with an SD of 1.59. Due to the presence of 1%, 2%, 4%, and 8% Pb, it shows a relatively linear decrease and was found to be 66.76 with an SD of 1.24, 55.75 with SD of 2.08, 51.77 with SD of 1.81 and 45.74 with SD of 1.35 respectively. This reduction is linked to the limited compatibility between lead and copper. Lead, being nearly insoluble in the Cu matrix, forms isolated, soft particles that do not contribute to mechanical reinforcement. These inclusions disrupt the uniform load distribution and reduce the alloy's resistance to indentation. As Pb content rises, the structural contribution of the copper phase diminishes, further weakening the material's hardness response [30,31].

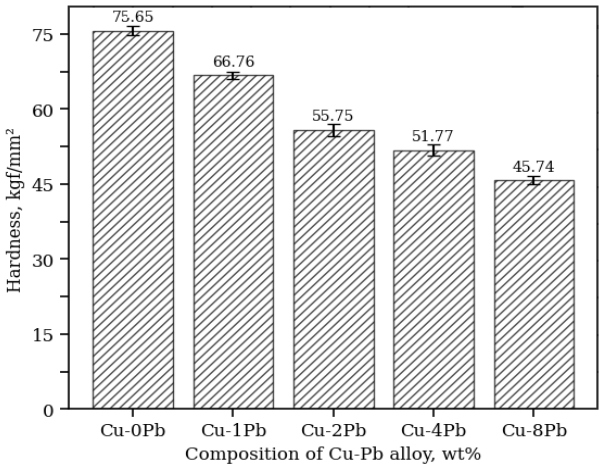

Fig. 5. Variation of materials micro-hardness for different compositions of Cu-Pb alloy

3.3. Leading Effect on Electrical Conductivity

The maximum electrical conductivity value is observed with no lead presence and is 59 MS/m. As the Pb presence increases to 1%, 2%, 4% and 8% the conductivity level decreases by 3.53%, 6.17%, 12.53%, and 18.64% respectively as shown in Fig. 6. It is noticed that the conductivity level does

not alter much with lower lead presence but varies drastically due to higher Pb content in pure Cu. This decline is attributed to the poor solubility of Pb in Cu, which leads to the formation of non-conductive lead particles. These particles disrupt the uniform metallic structure and act as scattering centers for conduction electrons, thereby reducing conductivity. While low Pb levels have a limited impact, higher concentrations introduce more scattering sites, significantly hindering electron flow. This behavior aligns with previous findings on impurity-induced conductivity loss in Cu-based alloys [32-34].

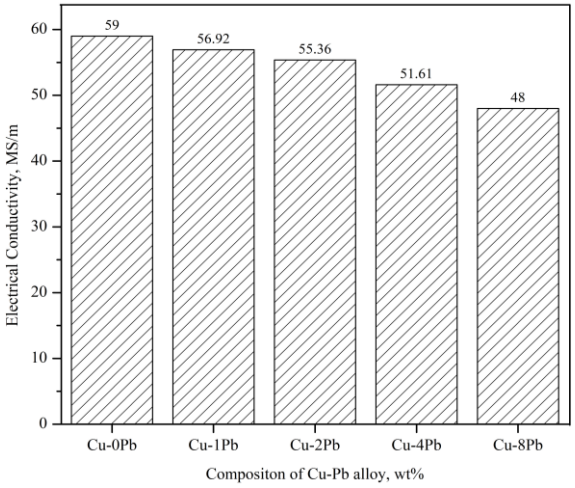

Fig. 6. Variation of materials electrical conductivity for different compositions of Cu-Pb alloy

3.4. Leading Effect on Corrosion Rate in Seawater

3.4.1. Weight Loss

There are differences in the mass loss amount per surface area exposed in the media for the immersion period amongst the sampling materials under varying lead content levels as seen in the table 1. All samples exhibit a similar pattern of weight loss as shown in Fig. 7, with the sharpest increase during the initial immersion period, indicating a more aggressive corrosion attack by seawater components.

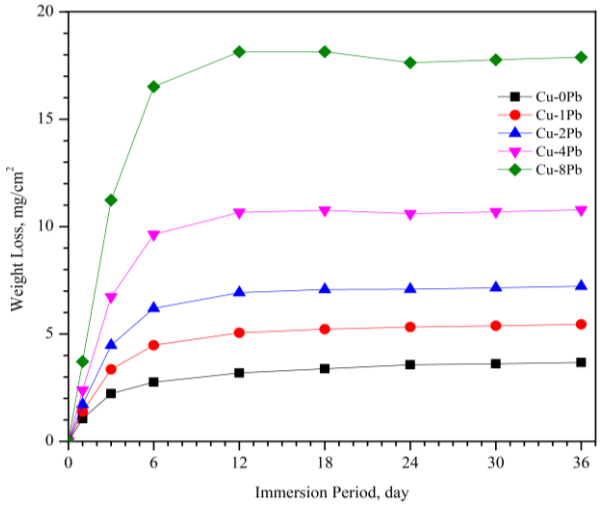

Fig. 7. Variation of materials weight loss for different compositions of Cu-Pb alloy due to corrosion in seawater

Over time, the mass loss tendencies reduce as a protective patina form, resulting in near-horizontal curves with minimal slope. (19,35) Cu-8Pb shows the highest mass loss, reaching 17.886 mg/cm^2 by 36 days, followed by Cu-4Pb (10.779 mg/cm^2), Cu-2Pb (7.225 mg/cm^2), Cu-1Pb (5.449 mg/cm^2), and Cu-0Pb (3.672 mg/cm^2). It is thus observed that the cumulative degradation of weight in seawater has been increased by 48.36% for Cu-1Pb, 96.74% for Cu-2Pb, 193.5% for Cu-

4Pb, and 387.2% for Cu-8Pb compared to pure copper (Cu-0Pb). These results highlight the significant influence of lead content on corrosion behavior, with higher lead levels drastically accelerating mass loss [35].

3.4.2. Corrosion Rate

The corrosion rate data for five copper-based samples (Cu-0Pb, Cu-1Pb, Cu-2Pb, Cu-4Pb, and Cu-8Pb) was analyzed over an immersion period of 36 days. The results illustrated in Fig. 8 indicate that all samples exhibited the highest corrosion rates after the first day of immersion, with values of 0.43013 mm/yr for Cu-0Pb, 0.56475 mm/yr for Cu-1Pb, 0.69814 mm/yr for Cu-2Pb, 0.96328 mm/yr for Cu-4Pb, and 1.48518 mm/yr for Cu-8Pb. These rates declined sharply with increasing immersion time, reflecting the formation of a protective patina that reduced the corrosion process. (19) By the end of 36 days, the corrosion rates were significantly reduced to 0.04165 mm/yr, 0.06166 mm/yr, 0.0815 mm/yr, 0.12094 mm/yr, and 0.19856 mm/yr for Cu-0Pb, Cu-1Pb, Cu-2Pb, Cu-4Pb, and Cu-8Pb, respectively. The data shows that the addition of lead content progressively increases the initial corrosion rates, with Cu-8Pb experiencing the highest rates throughout. However, the declining trend suggests that patina formation mitigates the adverse effects of higher lead content over time [36].

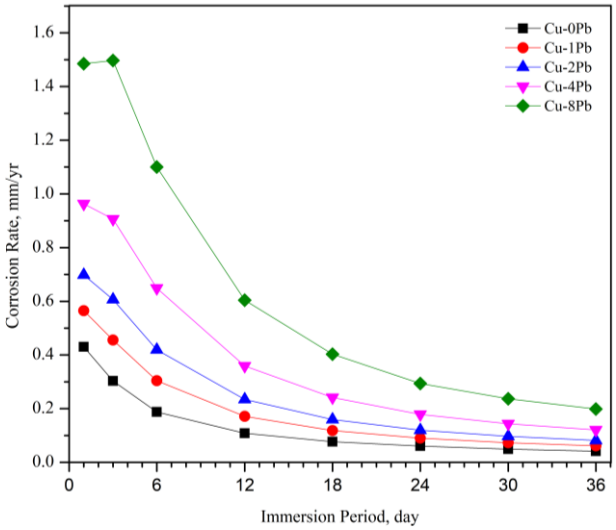

Fig. 8. Variation of materials corrosion rate for different compositions of Cu-Pb alloy due to corrosion in seawater

3.4.3. Average Corrosion Rate

The average values of corrosion rates for all five alloys are shown in the bar chart in Fig. 9. The chart demonstrates that Cu-8Pb has the highest average corrosion rate, followed by Cu-4Pb, Cu-2Pb, Cu-1Pb, and Cu-0Pb. Specifically, the average corrosion rates of these alloys are 0.62 mm/yr, 0.38 mm/yr, 0.26 mm/yr, 0.20 mm/yr, and 0.14 mm/yr respectively. This indicates a progressive increase in corrosion rates as the lead content in copper alloys increases [17,19].

Owing to the negligible solubility of Pb in the copper matrix, it precipitates as discrete soft particles that do not contribute to the formation of a continuous and adherent passive film [37]. These Pb inclusions interrupt the protective oxide layer and act as local galvanic sites, intensifying electrochemical activity in corrosive environments [38]. Consequently, corrosion tends to accelerate with increasing Pb content, compromising the alloy's suitability for marine or aggressive environments [37,39]. Therefore, Cu-0Pb shows the least corrosion, making it a highly effective material for applications where corrosion resistance is a key concern, especially in seawater environments.

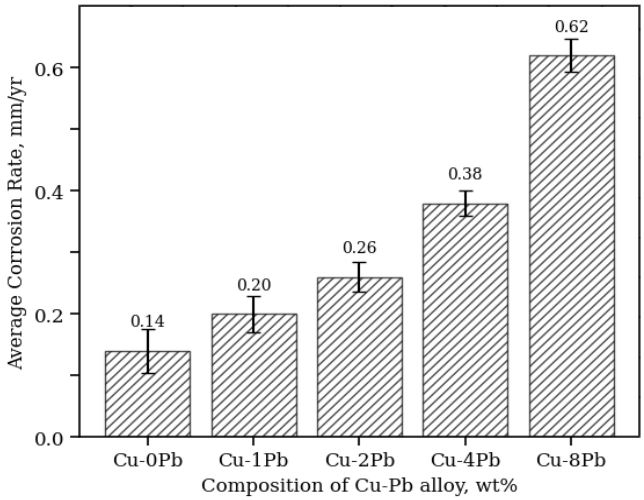

Fig. 9. Variation of materials average corrosion rate for different compositions of Cu-Pb alloy due to corrosion in seawater

3.5. Leading Effect on Electrical Conductivity in Seawater

The electrical conductivity of Cu-Pb alloys in seawater over various immersion periods is illustrated in Fig. 10 for all five samples. The initial measurements show that Cu-0Pb has the highest conductivity at 59 S/m, followed by Cu-1Pb, Cu-2Pb, Cu-4Pb, and Cu-8Pb with 56.92 MS/m, 55.36 MS/m, 51.61 MS/m, and 48.00 MS/m respectively [14]. As the immersion period progresses, the conductivity values of all alloys slightly decrease but remain relatively stable throughout the immersion period. After 36 days, Cu-0Pb maintains a conductivity of 59.71 S/m, while the alloys with higher lead content (Cu-1Pb, Cu-2Pb, Cu-4Pb, and Cu-8Pb) exhibit values of 57.02 MS/m, 55.05 MS/m, 51.68 MS/m, and 48.14 MS/m, respectively. The trends indicate that Cu-0Pb exhibits the most stable and highest conductivity throughout the immersion period, making it the most suitable material for applications where high electrical conductivity in seawater is crucial. As the lead content increases, conductivity decreases, with Cu-8Pb demonstrating the lowest conductivity, particularly after extended immersion.

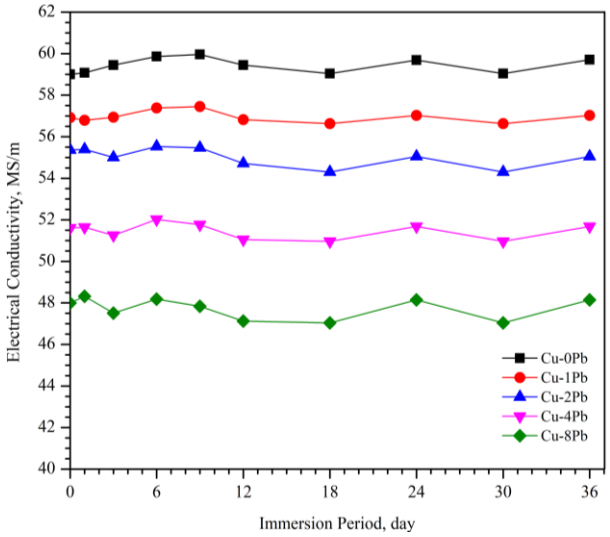

Fig. 10. Variation of materials electrical conductivity for different compositions of Cu-Pb alloy due to corrosion in seawater

3.6. Microstructure observation

3.6.1. Leading Effect on Micro-Structure–Optical Electronic Microscopic (OEM) Images

The OEM micrographs of all five-sample materials have been observed to investigate the variation in microstructures before and after etching into the solution. From Fig. 11 (i) fresh polishing marks are visible without any foreign particles in the grain boundaries [40]. From Fig. 11 (ii-v) the distributed presence of Pb is visualized as a solute in Cu solvent in contrast to Fig. 11 (i) which contributes to the alteration in micro-hardness, resistivity, and tensile behavior of the sample materials. The grain sizes are also observed to be varied clearly for all the cast alloys due to etching into the solution. It is noticed that there are definite changes in grain shape and grain boundary patterns [14]. Five such micrographs have been presented in Fig. 11 (vi-x). The dispersed Pb inclusions can enhance heterogeneous nucleation during solidification, contributing to the observed grain size reduction [1].

Figure (vii-ix) indicates that the lead atom is located in between the boundary of the grain, which is a consequence of grain boundary segregation due to Pb's poor solubility in Cu. This behavior arises from energetic preference and atomic size mismatch. The segregation leads to local distortion of the grain boundary region, influencing microstructural integrity and altering the alloy's mechanical and electrical behavior [41-43]. As the atom sizes are smaller, they can easily settle down in those locations and alter the lattice structure of copper atoms. Fig. 11 (x) shows as the lead presence is increased, the atoms of lead not only are placed to the grain boundary but also displace copper grain and occupy themselves as lead grain. This reshaping of grains may be attributed to the finding associated with electrical conductivity, in which the conductivity has decreased [44,45].

Unetched Samples

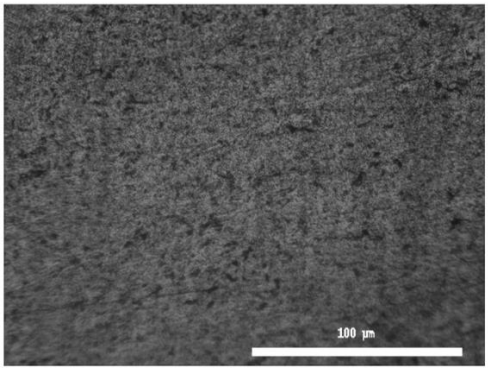

(i) Pure Cu

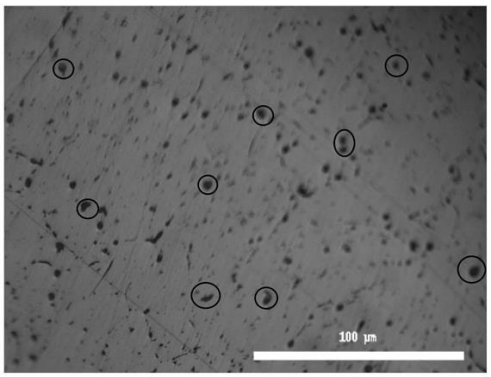

(ii) Cu-1Pb

Etched Samples

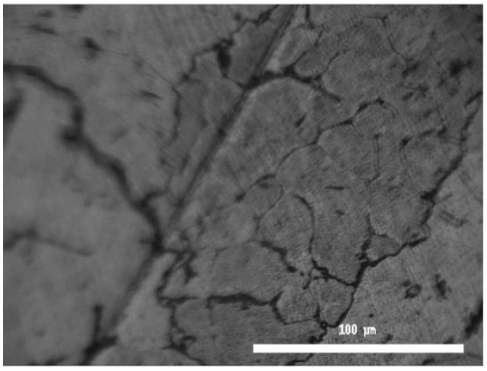

(vi) Pure Cu

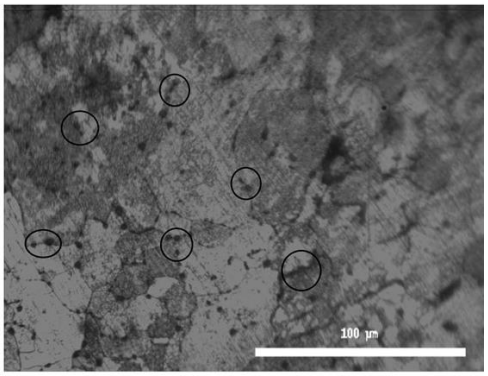

(vii) Cu-1Pb

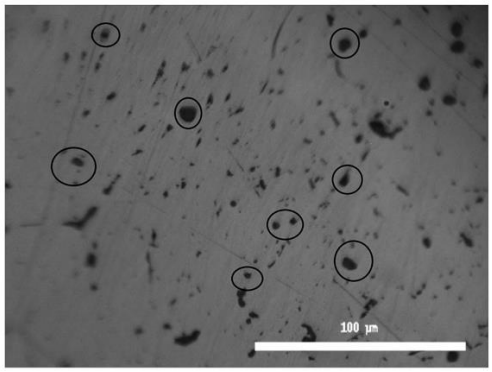

(iii) Cu-2Pb

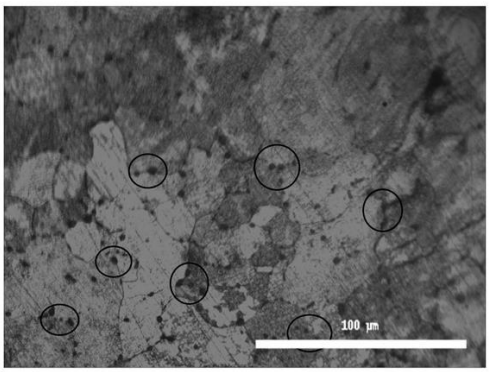

(viii) Cu-2Pb

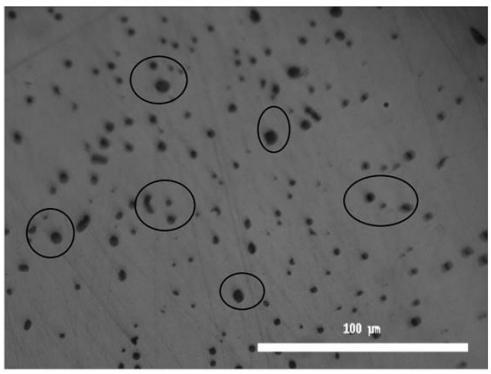

(iv) Cu-4Pb

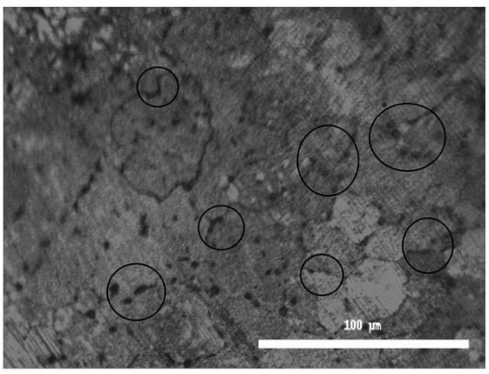

(ix) Cu-4Pb

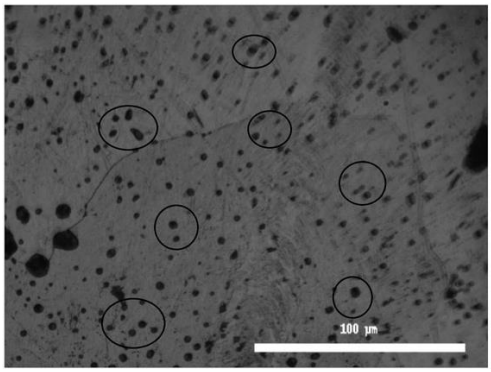

(v) Cu-8Pb

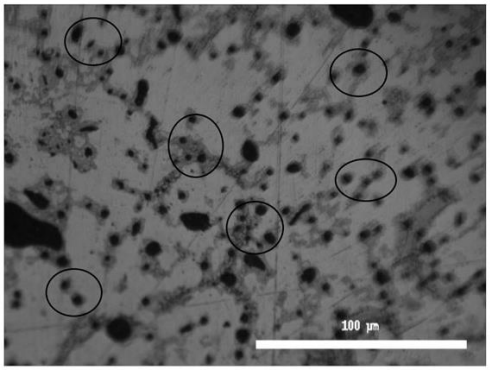

(x) Cu-8Pb

Fig. 11. Micro-structure(320x) of different compositions of Cu-Pb alloy samples

3.6.2. Corrosion Effect on Micro-Structure–Optical Electronic Microscopic (OEM) Images

The OEM images of all five sample materials are observed after submersion for 36 days in a seawater environment. The polishing marks have faded away from the sample surfaces due to the global corrosion effect which eventually indicates the weight loss and corrosion rate during gravimetric observation shown in Fig. 12. These figures indicate some pits in all five sample materials with randomly nucleated orientation; demonstrating that the samples have suffered from a pitting corrosion attack [10,46,47]. Fig. 12 (iv, v) has been found to be the darkest which confirms the analysis. Darker regions in the micrographs indicate extensive surface degradation due to pitting and oxide formation, which reduce light reflectivity. This visual trend aligns with the gravimetric results, confirming that samples in Fig. 12 (iv, v) experienced the most severe corrosion. Such a correlation between microstructural contrast and corrosion rate is well-supported in the literature [48-51].

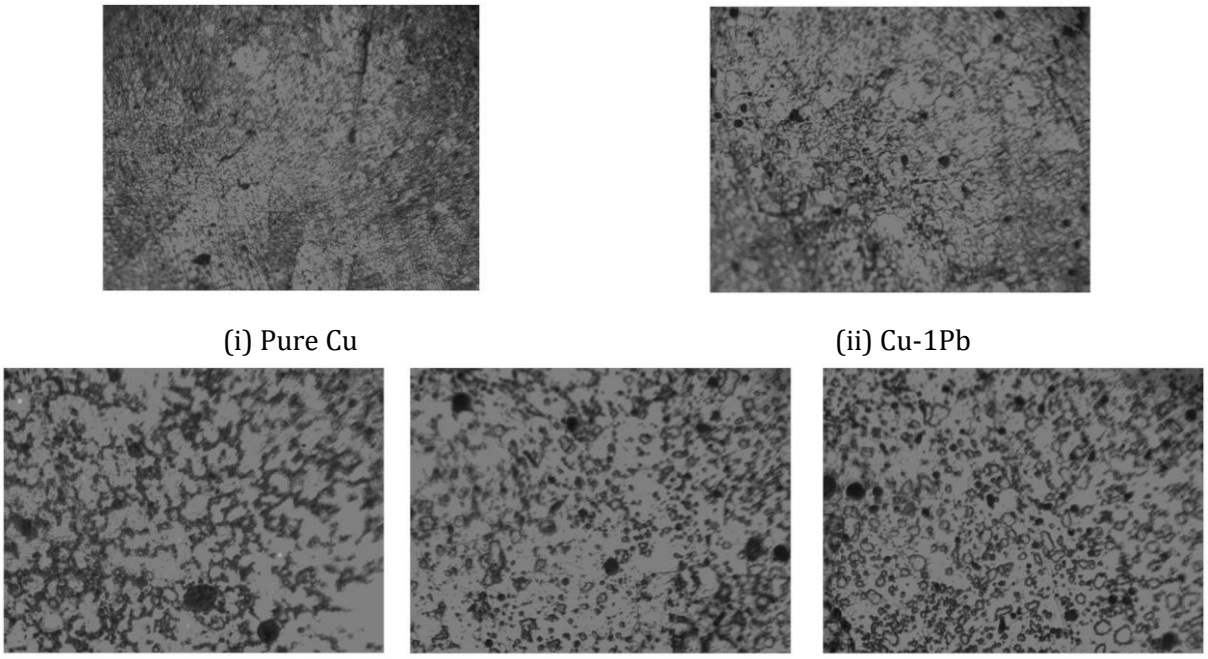

(i) Pure Cu (ii) Cu-1Pb

(iii) Cu-2Pb (iv) Cu-4Pb (v) Cu-8Pb

Fig. 12. Micro-structure(320x) of different compositions of Cu-Pb alloy samples after immersion into seawater for 36 days

4. Conclusions

A study was carried out to investigate the electromechanical and corrosive properties of copper in an attempt to assess the potential reuse of waste or wasted copper that is typically derived from old industries, buildings, and shipbreaking yards. This investigation considered the influence of trace Pb-solder additions on selected physical parameters, including tensile properties, material hardness, electrical conductivity, corrosive behavior, and microstructural characteristics.

All four leaded samples had significant changes in grain morphology, including variations in grain size, shape, and boundary features, according to the microstructural study. The main cause of these changes is lead, which serves as a microstructural modifier during solidification and the thermal processing that follows. The mechanical and physical properties of the materials were greatly impacted by these microstructure modifications. It was discovered that differences in grain structure and boundary configurations specifically affected micro-hardness. Similarly, the redistribution of lead-rich phases along grain boundaries, which probably interfered with electron flow, had an impact on electrical resistivity. Modified grain boundary cohesion and possible lead segregation at crucial points also had an impact on tensile characteristics, such as yield strength and elongation. Consequently, most mechanical properties were found to be influenced by the presence of lead. For example, even a little amount of lead content resulted in discernible decreases in yield strength and Young's modulus. On the other hand, total strain decreased significantly with decreasing lead content but was mostly constant as lead concentration rose. As lead levels increased, microhardness decreased almost linearly. In contrast, conductivity was not significantly affected at lower lead content (1–2%), making it suitable for preserving conductivity levels. After 36 days of exposure to seawater, conductivity fluctuations were minimal, while the corroded layer remained firmly adhered to the surface.

Seawater represents a chemically complex medium, influenced by factors such as pH, salinity, dissolved gases, conductivity, and various other parameters. Additionally, seawater composition can vary across different oceans, leading to diverse corrosion behaviors in copper alloys. Findings from this study conducted in the Bay of Bengal revealed that none of the five sample materials were entirely resistant to corrosion. Because of the development of patina on the materials' surface, corrosion rates were highest in the early phases and then dramatically dropped after that.

Comparing the studied copper samples to pure copper, those with higher lead contents showed noticeably higher corrosion susceptibility. Lead-rich phases served as preferred locations for localized corrosion, and the higher lead content promoted the development of micro-galvanic cells inside the copper matrix. During prolonged immersion, where the leaded alloys showed significant surface deterioration, pitting, and material loss, this behavior was most noticeable. On the other hand, under the same circumstances, pure copper showed better resistance to corrosion, retaining a more stable and protective oxide layer that prevented the corrosive medium from attacking further. These findings imply that lead reduces the overall corrosion resistance of copper alloys, even though it improves some other mechanical properties. Microstructural analyses of the corroded surfaces further corroborated the observed corrosiveness. These findings underscore the necessity of incorporating allowances for corrosion when designing products made from copper and its alloys for various marine applications.

References

[1] Davis JR. Copper and copper alloys. In: Alloying. 2001. p. 457-94. https://doi.org/10.31399/asm.tb.aub.t61170457

[2] Collini L. Copper alloys - early applications and current performance. InTech; 2012. p. 186. https://doi.org/10.5772/1912

[3] Villena M, Greve F. On resource depletion and productivity: the case of the Chilean copper industry. Resour Policy. 2018 Dec;59:553-62. https://doi.org/10.1016/j.resourpol.2018.10.001

[4] Cui J, Forssberg E. Mechanical recycling of waste electric and electronic equipment: a review. J Hazard Mater. 2003 May 30;99(3):243-63. https://doi.org/10.1016/S0304-3894(03)00061-X

[5] Fogarasi S, Imre-Lucaci F, Imre-Lucaci Á, Ilea P. Copper recovery and gold enrichment from waste printed circuit boards by mediated electrochemical oxidation. J Hazard Mater. 2014 May 30;273:215-21. https://doi.org/10.1016/j.jhazmat.2014.03.043

[6] Samuelsson C, Björkman B. Copper recycling. In: Handbook of Recycling: State-of-the-Art for Practitioners, Analysts, and Scientists. 2014. p. 85-94. https://doi.org/10.1016/B978-0-12-396459-5.00007-6

[7] Jones A, Lee R. Surface interactions between copper alloys and heavy metals in industrial environments. J Corros Sci. 2020;167:108520.

[8] Anand S, Srivatsan TS, Sudarshan TS. The influence of alloy composition on microstructure and tensile behaviour of copper-lead alloys. J Mater Sci. 1993;28:4615-22. https://doi.org/10.1007/BF00414249

[9] Paige JI, Covino BS Jr. Leachability of lead from selected copper-base alloys. Corrosion. 1992;48(12):1040-6. https://doi.org/10.5006/1.3315907

[10] Farro NW, Veleva L, Aguilar P. Copper marine corrosion: I. Corrosion rates in atmospheric and seawater environments of Peruvian port. Open Corros J. 2009;2:130-138. https://doi.org/10.2174/1876503300902010130

[11] Johnsen R. Experience with the use of copper alloys in seawater systems on the Norwegian Continental Shelf. In: Corrosion Behaviour and Protection of Copper and Aluminium Alloys in Seawater. 2007. p. 62-72. https://doi.org/10.1533/9781845693084.2.62

[12] Núñez L, Reguera E, Corvo F, González E, Vazquez C. Corrosion of copper in seawater and its aerosols in a tropical island. Corros Sci. 2005 Feb;47(2):461-84. https://doi.org/10.1016/j.corsci.2004.05.015

[13] Orozco-Cruz R, Ávila E, Mejía E, Pérez T, Contreras A, Galván-Martínez R. In situ corrosion study of copper and copper-alloys exposed to natural seawater of the Veracruz Port (Gulf of Mexico). Int J Electrochem Sci. 2017 Apr;12(4):3133-52. https://doi.org/10.20964/2017.04.27

[14] Rahman MM, Ahmed SR, Kaiser MS. On the investigation of reuse potential of SnPb-solder affected copper subjected to work-hardening and thermal ageing. Mater Charact. 2021 Feb;172:110878. https://doi.org/10.1016/j.matchar.2021.110878

[15] ASTM Standard E92-10. Standard test method for Knoop and Vickers hardness of materials. West Conshohocken, PA: ASTM International; 2010.

[16] Santos CIS, Mendonça MH, Fonseca ITE. Corrosion of brass in natural and artificial seawater. J Appl Electrochem. 2006 Oct;36(12):1353-9. https://doi.org/10.1007/s10800-006-9230-z

[17] Rahman MM, Ahmed R, Kaiser MS. Corrosion behavior of work hardened commercial copper alloys in the Bay of Bengal water environment. Khulna; 2020.

[18] Rahman MM, Ahmed SR. Corrosion behavior of copper-based heat exchanger tube in waters of Bangladesh region at varied temperature and flow velocity. MIST Int J Sci Technol. 2020 Dec;8:15-23. https://doi.org/10.47981/j.mijst.08(02)2020.196(15-23)

[19] Rahman MM, Ahmed SR, Kaiser MS. Corrosion behavior of work hardened SnPb-solder affected copper in the Bay of Bengal water environment. Adv Mater Sci Eng. 2022;2022:1-14. https://doi.org/10.1155/2022/2513391
[20] Al-Qudah MA, Al-Rawashdeh N, Al-Abdallah MM, Maayta AK, Al-Qudah MA, Al-Rawashdeh NAF. Corrosion behavior of copper in chloride media. Open Corros J. 2009;2:71-6. https://doi.org/10.2174/1876503300902010071
[21] Culpan EA, Rose G. Corrosion behaviour of cast nickel aluminium bronze in sea water. Br Corros J. 1979 Jan;14(3):160-6. https://doi.org/10.1179/bcj.1979.14.3.160
[22] Baboian R. Corrosion tests and standards: application and interpretation. ASTM International; 2005. https://doi.org/10.1520/MNL20_2ND-EB
[23] Hassan SF, Gupta M. Development of high performance magnesium composites using nano-sized and micron-sized reinforcements. J Mater Process Technol. 2005;162-163:58-63.
[24] Ahamed A, Das D. Influence of Bi and Pb on microstructure and mechanical properties of copper alloys. Mater Sci Eng A. 2016;660:68-76.
[25] Wang W, Li R, Hu W. Interfacial behavior and mechanical properties of Cu-Pb alloys. J Alloys Compd. 2013;578:288-93.
[26] Chen W, Li Z, Zhou Y. Effect of particle size and content of Pb on mechanical properties of Cu-Pb alloys. Mater Des. 2010;31(2):918-22.
[27] Zaki AI, Megahed MM. Microstructure and mechanical behavior of copper-lead alloys for bearing applications. Mater Des. 2015;65:823-30.
[28] Moridi M, Behnia AM, Khosroshahi R. Effects of soft phase inclusions on the mechanical behavior of metal matrix composites. J Mater Eng Perform. 2014;23(6):2136-43.
[29] Yuan Z, Cheng Y, Zhao J. Effect of non-metallic inclusions on fatigue and fracture properties of metal matrix systems. Metals. 2019;9(8):897.
[30] Wang X, Gao B, Zhang Y, Ma X. Effects of lead addition on microstructure and mechanical properties of copper alloys. Mater Sci Eng A. 2018;732:130-8.
[31] Zhang T, Liu Y, Chen Y, Wu S. Influence of insoluble phase distribution on mechanical behavior of copper-based alloys. J Alloys Compd. 2021;855:157487.
[32] Kim JS, Lee HW, Choe HC. The electrical and mechanical properties of Cu-Pb alloy with Pb content. Mater Sci Eng A. 2007;449-451:819-22. https://doi.org/10.1016/j.msea.2006.02.326
[33] Li H, Ma Y, Wang Y. Influence of Pb on the microstructure and electrical properties of copper matrix composites. J Alloys Compd. 2012;540:121-6.
[34] Ahn SH, Kang SK, Kwon H. Effect of Pb on the electrical and mechanical properties of Cu alloys for electronic components. J Mater Sci Mater Electron. 2000;11(4):293-7.
[35] Arjmand F, Adriaens A. Influence of pH and chloride concentration on the corrosion behavior of unalloyed copper in NaCl solution: a comparative study between the micro and macro scales. Materials (Basel). 2012 Nov;5(12):2439-64. https://doi.org/10.3390/ma5122439
[36] Rahman MM, Chowdhury RH, Rafi TA, Ahmed SR. Corrosion resistance of scraped copper in velocity varied inland water of Bangladesh. Malays J Compos Sci Manuf. 2024 Mar;13(1):25-35. https://doi.org/10.37934/mjcsm.13.1.2535
[37] Peng DQ, Ke W, Dong CF. Effect of Pb on corrosion behavior of Cu alloys in seawater. Corros Sci. 2009;51(3):526-34.
[38] Pourbaix M. Atlas of electrochemical equilibria in aqueous solutions. Houston: NACE Int.; 1974.
[39] Abd El Rehim SA, Hassan HH, Mohamed NF. Electrochemical behavior of copper in chloride solutions and its corrosion inhibition by some amino acids. Mater Chem Phys. 2001;70(1):64-72. https://doi.org/10.1016/S0254-0584(00)00468-5
[40] Bernal JD. The complex structure of the copper-tin intermetallic compounds. Nature. 1928;122(3063):54. https://doi.org/10.1038/122054a0
[41] Wang H, Wang C, Liu C, Yang Y, Liu Z, Zhang Z. Grain boundary segregation and embrittlement in metallic alloys. Prog Mater Sci. 2015;71:1-49.
[42] Choi P, Borchers C, Richter A, et al. Atomic-scale analysis of solute segregation at grain boundaries in metallic alloys. Acta Mater. 2010;58(7):2310-23.
[43] Randle V. Mechanisms of grain boundary segregation and their effects on intergranular corrosion. Corros Sci. 2004;46(1):211-25.
[44] Gupta SP, Rathor D. Kinetics of growth of intermetallics in the Cu-Sn system. Int J Mater Res. 2002 Jun;93(6):516-22. https://doi.org/10.3139/146.020516
[45] Fujiwara H, Nishimoto T, Miyamoto H, Ameyama K. Microstructure and mechanical properties of Cu-Sn alloy with harmonic structure. In: Proc 8th Pacific Rim Int Congr Adv Mater Process. 2013. p. 2455-60. https://doi.org/10.1007/978-3-319-48764-9_304
[46] Kuźnicka B, Junik K. Intergranular stress corrosion cracking of copper - a case study. Corros Sci. 2007 Oct;49(10):3905-16. https://doi.org/10.1016/j.corsci.2007.05.014

[47] Zhang YN, Zi JL, Zheng MS, Zhu JW. Corrosion behavior of copper with minor alloying addition in chloride solution. J Alloys Compd. 2008 Aug;462(1-2):240-3. https://doi.org/10.1016/j.jallcom.2007.08.008
[48] Fontana MG. Corrosion engineering. 3rd ed. New York: McGraw-Hill; 1986.
[49] Zhang X, Wu H, Liu G, Hu J. Effect of seawater environment on corrosion behavior of different metals. J Mater Res Technol. 2017;6(4):362-8.
[50] Subramanian B, Ravichandran K, Narayanasamy B. Correlation between corrosion rate and optical/electron microscopy features. J Rare Earths. 2008;26(5):673-6.
[51] Wang L, Li X. Morphological and microstructural characteristics of pitting corrosion in steels. J Mater Sci Technol. 2019;35(9):1987-95.